NASA TECHNICAL TRANSLATION NASA TT F-14,074

CALCULATION PROCEDURES FOR THREE-DIMENSIONAL AERODYNAMICS IN PERFECT FLUIDS

P. Perrier and W. Vitte

Translation of "Elements de Calcul d'Aérodynamique Tridimensionnelle en Fluide Parfait", Avions Marcel Dassault, Paper presented to the Association Francaise des Ingeniurs et Téchnicians de l'Aérnautique et de l'Espace, 7th Aérodynamics Colloquiem, Modane and Ecully, France, November 4-6, 1970, 39 pages.

N72-12982 (NASA-TT-F-14074) CALCULATION PROCEDURES FOR THREE DIMENSIONAL AERODYNAMICS IN PERFECT FLUIDS P. Perrier, et al (Scientific Translation Service) Dec. 1971
Unclas 11455 33 p CSCL 01A G3/01

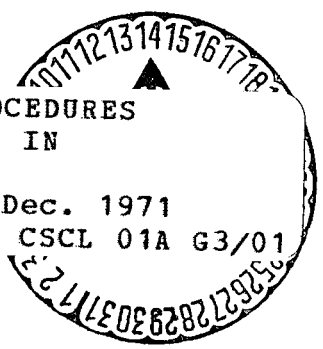

NATIONAL AERONAUTICS AND SPACE ADMINISTRATION
WASHINGTON, D. C. 20546 DECEMBER 1971

Reproduced by
NATIONAL TECHNICAL
INFORMATION SERVICE
U S Department of Commerce
Springfield VA 22151

TABLE OF CONTENTS

CALCULATION PROCEDURES FOR THREE-DIMENSIONAL AERODYNAMICS IN PERFECT FLUIDS

P. Perrier and W. Vitte

ABSTRACT. The three-dimensional problem of vortex interaction and its effect on lift, drag and other aerodynamic properties of various wing and aircraft configurations is treated by a new analytical method. The aerodynamic surfaces are replaced by equivalent surface elements. The data are displayed on an IBM terminal.

/1*

SUMMARY

This paper first reviews various problems of complete three-dimensional aircraft calculations. The importance of the vortex field on the local flow is demonstrated, which can be correctly calculated under subsonic flow conditions. It can be calculated approximately for transonic conditions and more precisely under supersonic conditions. Then the detailed study of the three-dimensional incompressible flow around a thin wing is developed. A numerical iteration method is used which makes it possible to establish the circulation surface over the wing and then to follow the evolution of the vortex sheet.

The non-linear effects caused by the rolling up effects at the tip and at the flap ends appear in the results of the calculation of the lift coefficient. The results obtained are in agreement with experiment.

The consequences of the discontinuity caused by the flaps at the engine level, on the rolling up of the vortex sheet, on the deflection field at the level of the empennage, and on the longitudinal stability of the aircraft are given by means of practical examples of using the method.

*Numbers in the margin indicate pagination in the original foreign text.

1. GENERAL REMARKS /4

The cost of developing an aircraft has become so high that construction cannot begin until a large number of tests in wind tunnels and a large number of calculations have been performed, which are designed to eliminate a large part of the uncertainties before flight. Simulation in the wind tunnel is not always possible because it is impossible to reproduce all the important similarity parameters (Mach number, Reynolds number, turbulence). Therefore, the calculation must provide a justification for transposing wind tunnel test results to flight conditions. Sometimes this evaluation is a better one than can be hoped for under actual flight conditions. In this case, the validity of some of the calculations will be justified by applying them to the reconstruction of wind tunnel tests of aircraft being studied or to aircraft which have already been built.

In such a reconstruction, the calculation of the so-called "linear" quantities such as the lift and stability curves, or the "parabolic" quantities, such as the drag curves, are only of secondary interest and limited to the stage before the project stage. During the "project" stage, the deviations with respect to these simplified models will be studied in detail. The greatest part of the aerodynamic study effort will be concentrated on these topics in order to define the aircraft.

Except for certain nonlinear quantities which can be calculated for a purely two-dimensional flow and which can be properly introduced in the calculation of an aircraft having a large sweepback and aspect ratio, almost all the non-linearities of an aircraft are of a three-dimensional nature. /5

The calculation of the complete configuration of an aircraft in the linear subsonic and supersonic regions can now be performed using a computer to a sufficient degree of accuracy. The corresponding methods of singularities distributed over the surface of the aircraft are now well known. However, there are problems associated with these methods. The calculation duration

extends over several hours on a large capacity computer. Sometimes the use of the computer is restricted, and more recently partial study methods are being used. In these, the small interactions of distant components are taken into account instead of carrying out a more refined analysis of the local problem. For example, the wing with fuselage or nacelle are treated in a schematic way, etc. This procedure leads to the development of a large number of computation programs which are simpler than the more refined and expensive ones. The latter are used as a last resort when the calculation is far enough along, and when the problem requires them. Computer time can be saved by providing programs which do not take the non-linearities into account except for second order solutions. In particular these make it possible to treat the three-dimensional transonic problem for a total number of iterations which is acceptable.

We will use a similar method for the calculations to be developed below, where we will limit ourselves to the interaction of free vortices with the lift. It will be seen that the calculation method used, which is the one due to Bielotserkovskiy [1], is very powerful and that it makes it possible to take into account three-dimensional and non-linear effects which is essential for the study of large incidence angles at low velocities. The free vortex sheet produced in this way influences the lift of the airfoil itself and also influences the aircraft empennage. The latter is often an amplifier of the irregular features of the vortex sheet. We will study these two non-linear sources in succession.

2. PROBLEM OF VORTEX INTERACTIONS ON THE LIFT /6

2.1. Exposition of the Method

2.1.1. Circulation Equation

Let us consider a thin wing of arbitrary cross sectional shape. The leading and trailing edges can be curved and can have angular points. The

method will be explained for the simple case of a wing having no wing flap system.

The vortex sheet is broken down in the following ways. We will first define the wing regions located between two breaks of the leading edge or of the trailing edge. Each region is then cut into equidistant bands, the number of which can vary from one region to another.

We will then define square elements by selecting cuts in the chord direction. This cut is done in the same way for all the regions.

The automatic meshing procedure places a lateral vortex on each square element, and a longitudinal vortex along the boundary between two square elements. The vortex sheet extends in the direction of the wind at infinity along the trailing edge of the wing and at the wing tip. Figure 2-1.1 shows an example of this meshing procedure. We therefore have a connected vortex system and two systems, 1 and 2, of free vortices. We will then define checkpoints located at the center of the vortex squares.*

The vortex nodes, the square elements and the checkpoints are defined by two indices J and K. J varies with X; K varies with Y. /7

We will first attempt to determine the circulation surface C (J, K), at each checkpoint which is generated by the vortex sheet.

Let us recall that a rectilinear vortex $\vec{A1A2}$ having the intensity Γ induces at a point M of space an induced velocity $\vec{W}$ given by the equation:

$$\vec{W} = \frac{1}{4\pi} \frac{\cos\alpha 1 + \cos\alpha 2}{} \Gamma \frac{\vec{A1A2} \wedge \vec{A1M}}{|A1A2 \wedge A1M|}$$

*Translator's Note: Numerous words in this paragraph and throughout the article are illegible.

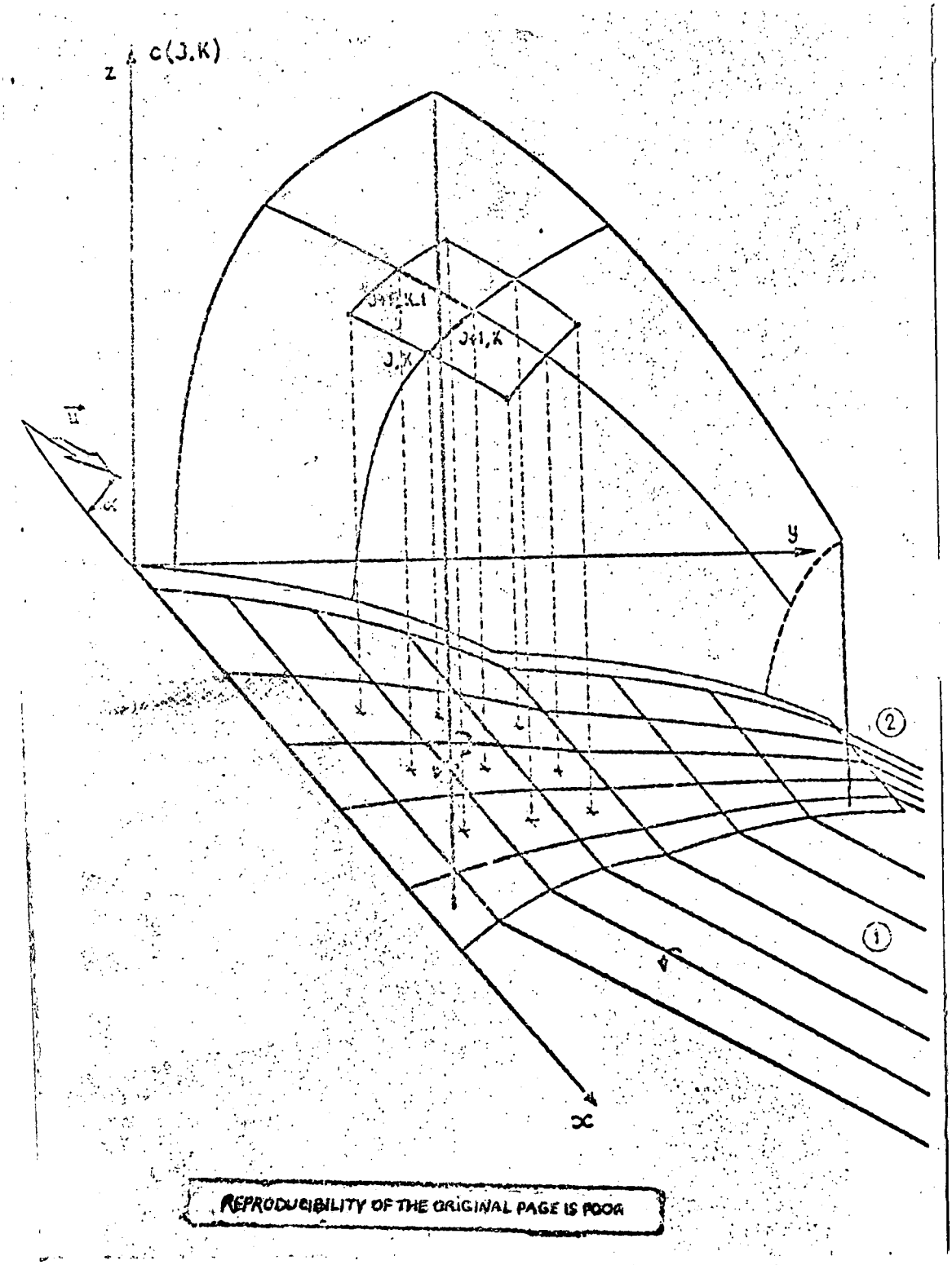

Figure 2.1.1. Representation of the vortex sheet. Circulation surface.

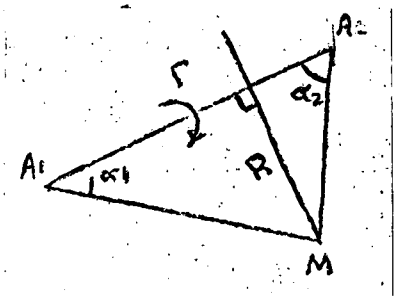

The intensity of each vortex is the difference in circulation of the two square elements which have the common boundary.

We will call $\Delta\vec{W}$ the influence of a vortex and (*) its symmetric counterpart.

At each checkpoint, we will calculate the velocity induced by the various vortex systems.

$\vec{W}_L$ system of longitudinal vortices /8

$\vec{W}_\Gamma$ system of lateral vortices

$\vec{W}_4$ system of free vortices 1

$\vec{W}_2$ system of free vortices 2

$$\vec{W} = \vec{W}_L + \vec{W}_\Gamma + \vec{W}_4 + \vec{W}_2 + \vec{U}_\infty$$

We will now write down the tangency condition at the wing. $\vec{N}(I)$ is the normal at the checkpoint I.

$$\vec{W} \cdot \vec{N}(I) = 0$$

The circulation equation in non-dimensional variables is obtained as follows:

$$\sum_{K=1}^{N}\sum_{J=1}^{M}\left(c(J+1,K)-c(J,K)\right)\Delta\vec{\omega}_{J,K}^{J,K+1}\cdot\vec{N}(I)+$$

$$\sum_{K=2}^{N}\sum_{J=1}^{M}\left(c(J+1,K-1)-c(J+1,K)\right)\Delta\vec{\omega}_{J,K}^{J+1,K}\cdot\vec{N}(I)+$$

$$\sum_{K=2}^{N}\sum_{J=M+1}^{M+N1}\left(c(M+1,K-1)-c(M+1,K)\right)\Delta\vec{\omega}_{J,K}^{J+1,K}\cdot\vec{N}(I)+$$

$$\sum_{J=1}^{M}\sum_{K=N+1}^{N+N2}\left(c(J+1,N)-c(J,N)\right)\Delta\vec{\omega}_{J,K}^{J,K+1}\cdot\vec{N}(I)=$$

$$-4\pi\vec{U}_\infty\cdot\vec{N}(I)$$

*Translators Note: Illegible.

which can be written as

$$\sum_{K=1}^{N} \sum_{J=1}^{M+1} \vec{A}(J,K) \cdot \vec{N}(1)\, C(J,K) = -\vec{U}_{\infty} \cdot \vec{N}(1)$$

with $C(1, K) = 0 \quad \forall K$

We obtain a system of M x N linear equations. We will solve them in order to find the surface C (J, K). /9

The first iteration of the calculation establishes the connected vortex sheet and the free vortex sheet which extends through infinity in the direction of $\vec{U}_{\infty}$. This model makes it possible to find the circulation surface. From it, the calculation proceeds by considering a checkpoint along each free vortex. The direction of the induced velocity vector is calculated at this point. A vortex element is placed at each control vortex which has the direction of the induced velocity vector for the entire sheet. A vortex element of infinite length having the direction of the wind at infinity is added to this.

Each new iteration recalculates the circulation surface and is added to the vortex sheet.

In the numerical programming of this method, particular care must be given to the selection of the free and connected vortex elements in order to avoid excessive computational time. Also a proper accuracy must be achieved.

2.1.2. Calculation of the Lift and of the Moment

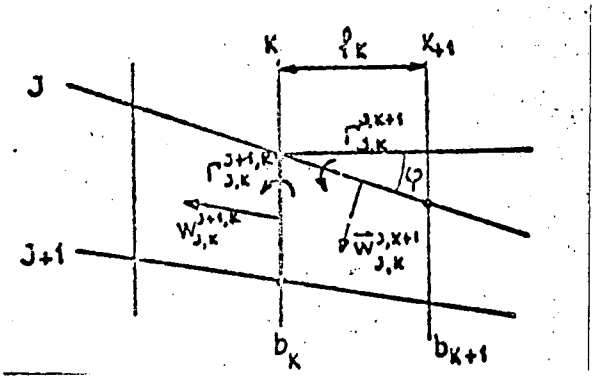

Let us consider a square element and calculate the elementary lift. /10

The difference in pressure between the bottom and top sides is given by the equation:

$$p_- - p_+ = \rho W \gamma^*$$

γ^* is the circulation per unit length which is uniformly distributed.
W is the velocity component at the point of calculation and perpendicular to the vortex axis. The other component does not induce any lift.

$$\Delta p = \frac{p_- - p_+}{\frac{1}{2}\rho U^2} = 2 \frac{W}{U} \gamma$$

From this, we obtain two contributions from each square element:

$$\Delta p^{J,K+1}_{J,K} = 2 \frac{W^{J,K+1}_{J,K}}{U} \gamma^{J,K+1}_{J,K}$$

$$\Delta p^{J+1,K}_{J,K} = 2 \frac{W^{J+1,K}_{J,K}}{U} \gamma^{J+1,K}_{J,K}$$

The Γ are the elementary vortex circulations which correspond to a "volume" of γ

$$\Gamma^{J,K+1}_{J,K} = \gamma^{J,K+1}_{J,K} \frac{b_K + b_{K+1}}{2b} \cos \varphi^{J,K+1}_{J,K}$$

$$\Gamma^{J+1,K}_{J,K} = \gamma^{J+1,K}_{J,K} \frac{\ell_K + \ell_{K+1}}{2b}$$

The lift coefficient will be given by: /11

$$C_z = \Sigma\Sigma \frac{\Delta p \, \Delta s}{S}$$

In the case of a planar wing, the components $W^{J,K+1}_{J,K}$ and $W^{J+1,K}_{J,K}$ are due to the vortices which escape at the wing tip and along the trailing edge. It follows that:

$$Cz = 2 \frac{B(1)}{\text{SURFACE}} \sum_{K=2}^{N} \sum_{J=1}^{M} \left[\left(\cos\alpha + \frac{W^{J,K+1}_{J,K,x1}}{U} + \frac{W^{J,K+1}_{J,K,x2}}{U} \right) \right.$$

$$\left(c(J+1,K) - c(J,K) \right) \Delta L - \left(\frac{W^{J,K+1}_{J,K,y1}}{U} + \frac{W^{J,K+1}_{J,K,y2}}{U} \right)$$

$$\left(c(J+1,K) - c(J,K) \right) \left(XT(J,K+1) - XT(J,K) \right) -$$

$$\frac{1}{2} \left(\frac{W^{J+1,K}_{J,K,y1}}{U} + \frac{W^{J+1,K}_{J,K,y2}}{U} \right) \frac{c(J+1,K-1) - c(J+1,K)}{M} B(K)$$

$$\left. - \frac{1}{2} \left(\frac{W^{J+1,K+1}_{J,K+1,y1}}{U} + \frac{W^{J+1,K+1}_{J,K+1,y2}}{U} \right) \frac{c(J+1,K) - c(J+1,K+1)}{M} B(K+1) \right]$$

The moment coefficient will be given by a similar expression. Only the distances X to the reference point for the moment must be given for each square element.

2.2. Calculation Example /12

2.2.1. Wing with Small Aspect Ratio

We recalculated the case of a wing having a constant chord with aspect ratio 1. Figure 2.2.1.1. shows the way in which the vortices found by the iterative calculation roll off the wing. In spite of the low number of points and iterations, the way in which the sheet rolls off the wing tip can be seen clearly. The increase of Cz as a function of incidence is given in Figure 2.2.1.2. It agrees well with the experimental Cz shown on the same figure and differs considerably from the linearized Cz found from the lifting surface theory, as well as from values obtained assuming that the sheet rolls off completely or is planar. Figure 2.2.1.3. corresponds to a Delta wing (MIRAGE III).

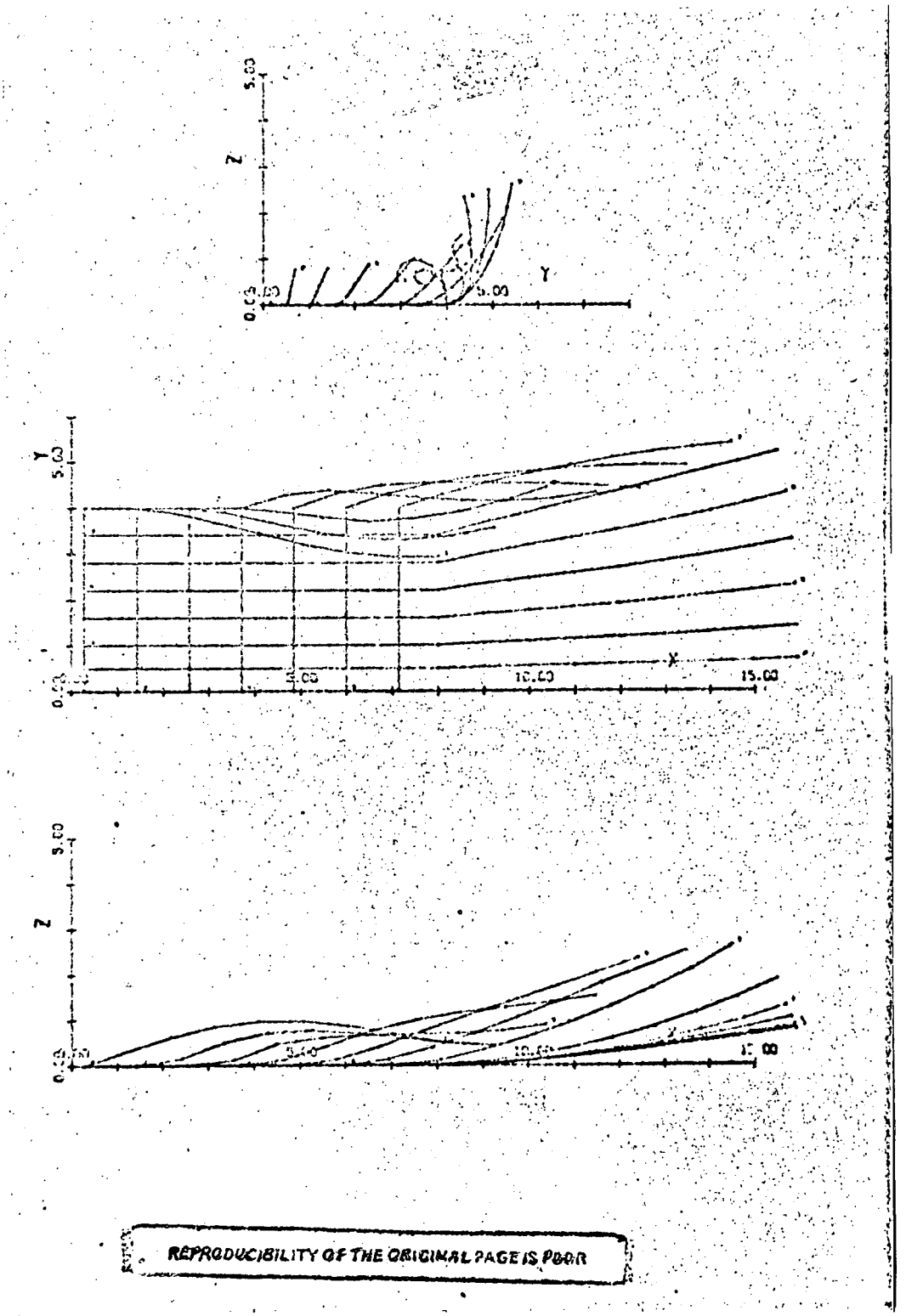

REPRODUCIBILITY OF THE ORIGINAL PAGE IS POOR

Figure 2.2.1.1. Flat plate: aspect ratio = 1, incidence 10°.

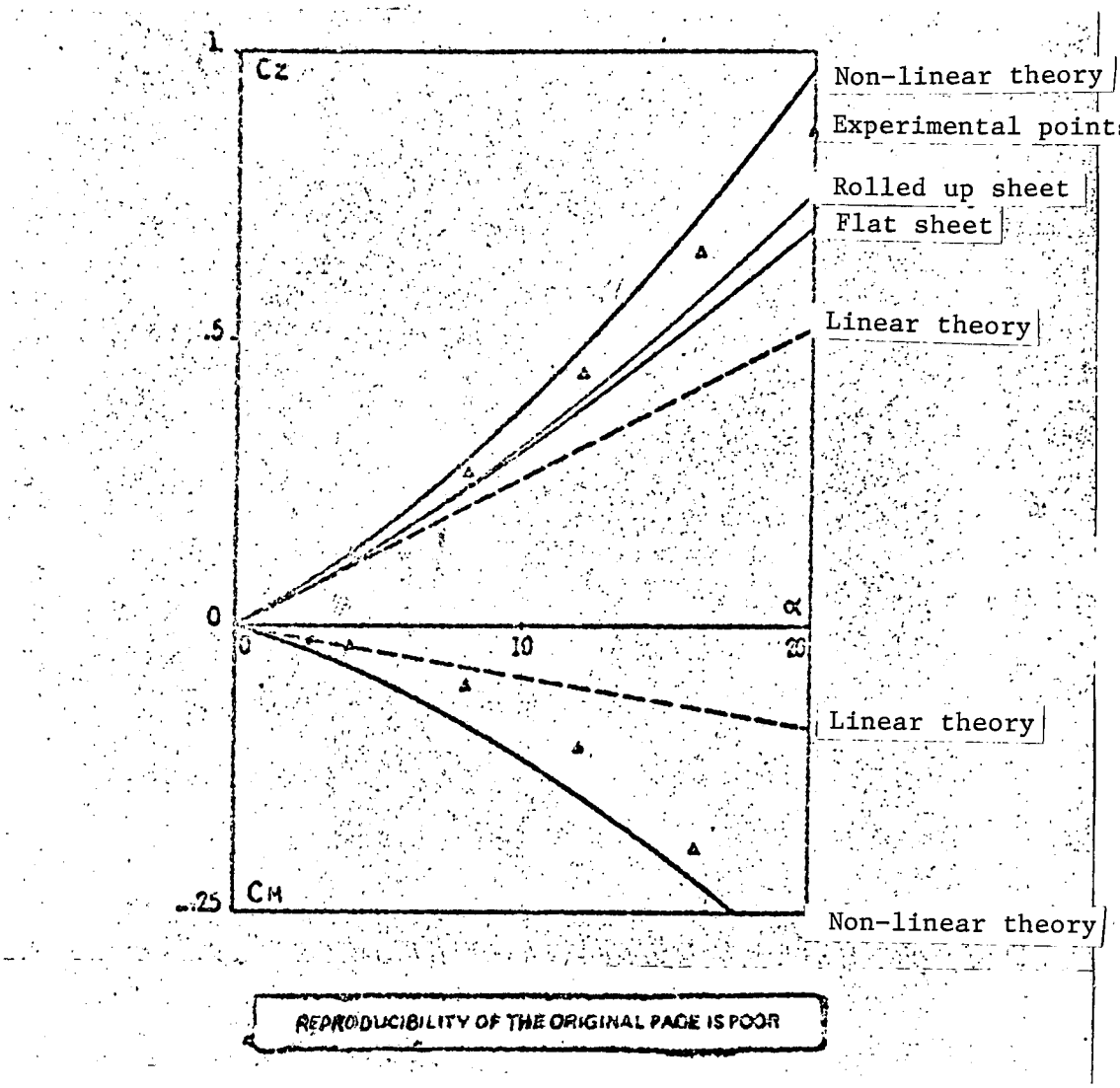

Figure 2.2.1.2. Curve for lift coefficient as a function of incidence, flat plate of aspect ratio 1.

2.2.2. Application to the Case of a Single Wing

Figure 2.2.2. shows a diagram of the vortices and the development of the free vortex sheet for the Mercury wing. The rolling off process at the wing tip is clearly indicated. In addition, the curve showing the circulation distribution in the span direction is similar to the one given by other aerodynamic methods. For this case, we studied the influence of the number of vortices leaving the wing tip. The chord distribution is not very sensitive to this parameter. In addition, it stabilizes at the end of a small number of

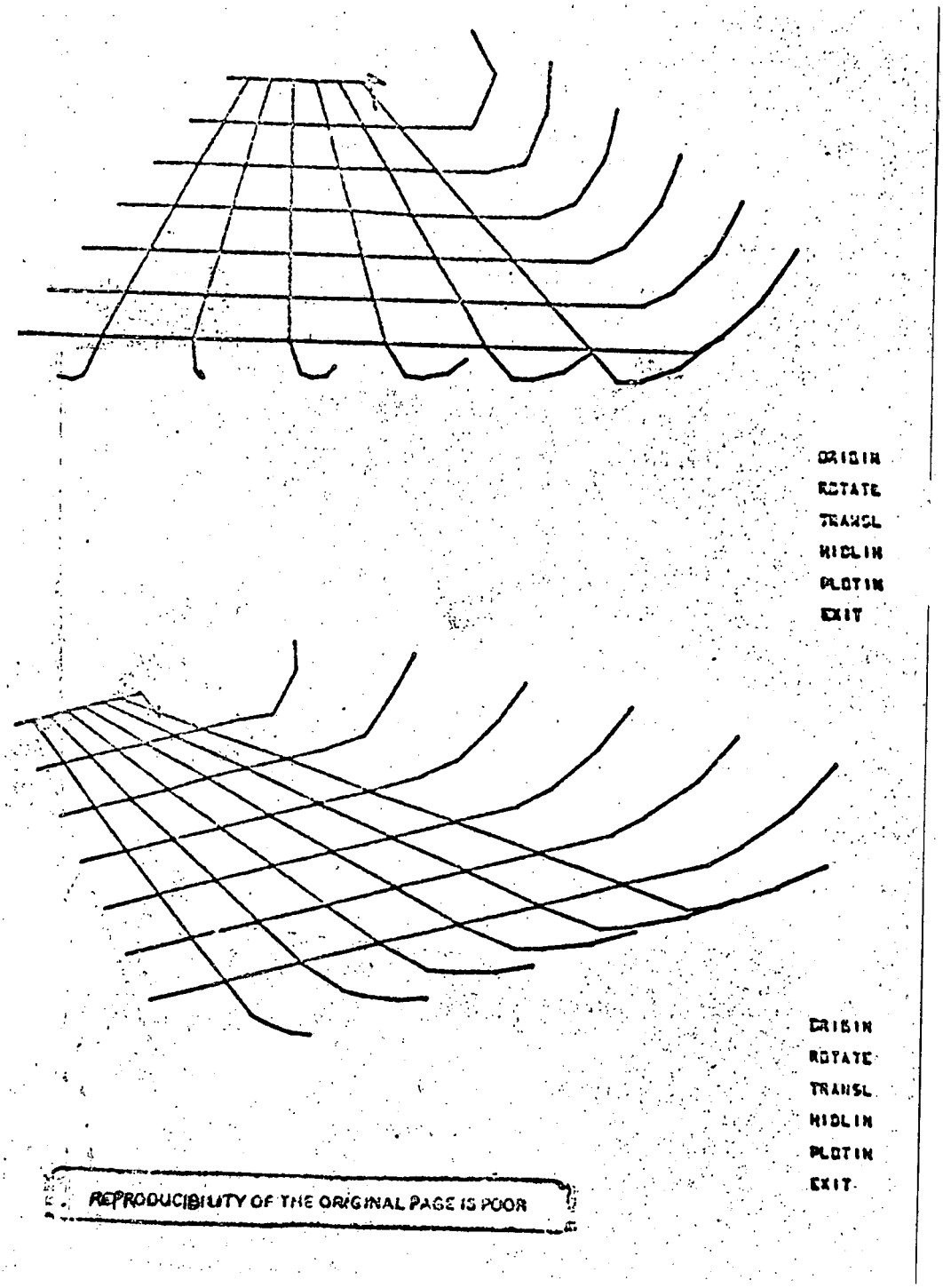

REPRODUCIBILITY OF THE ORIGINAL PAGE IS POOR

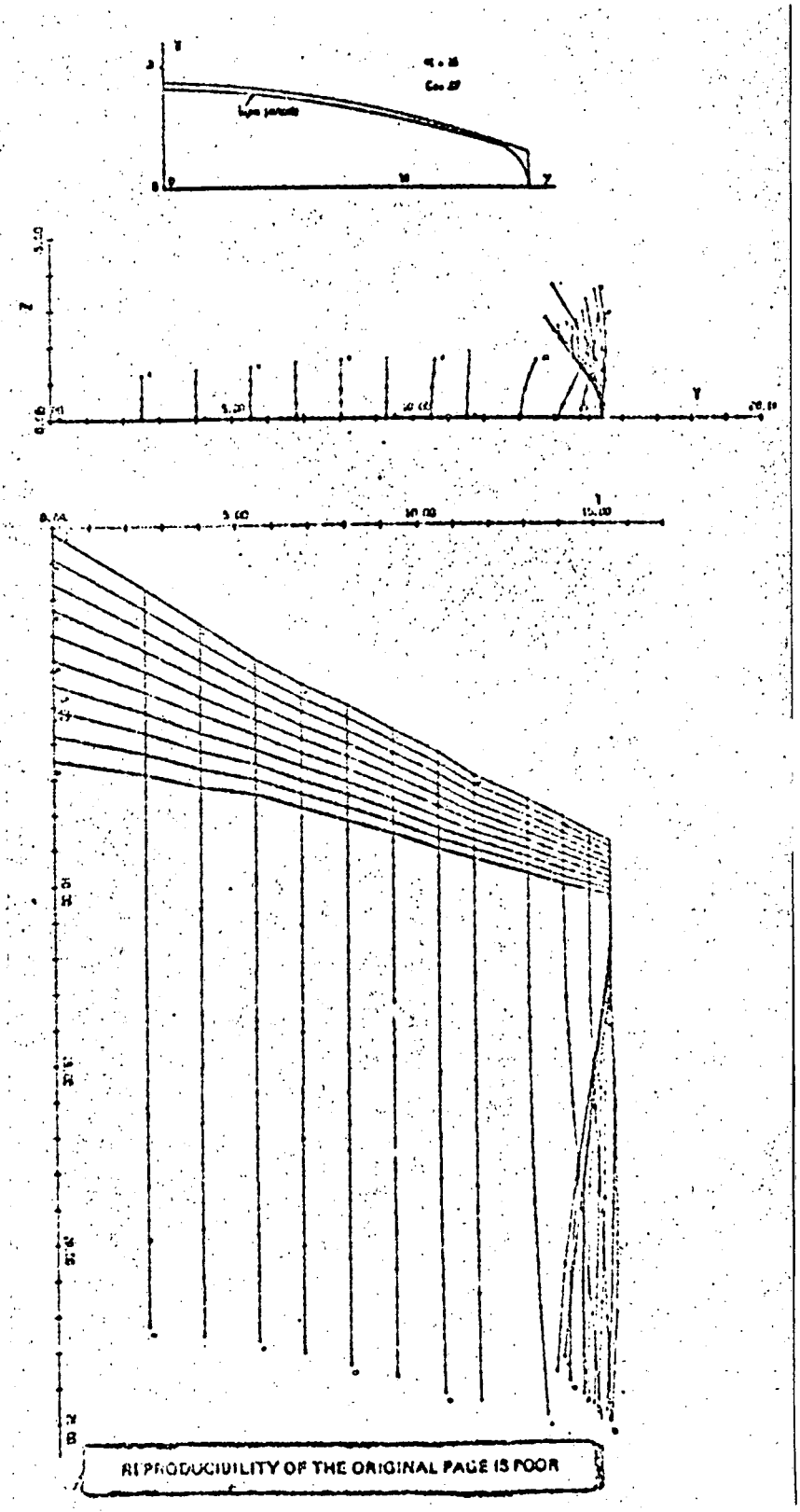

Figure 2.2.2. Mecury type wing: incidence 10°.

iterations. The step obviously has the greatest effect on this rolling off mechanism. It is also necessary to verify that it remains sufficiently small for a variation of the induced angles.

2.2.3. Wing with Flap

/13

We generalize the preceding method to the case of a wing having a continuous flap. The meshing procedure was therefore extended over the flap. The same rules were used and a vortex system at the end of the flap was introduced. The tangency condition was rewritten, this time taking into account the three components of the induced velocity vector. This calculation showed that there was a rolling off from the flap end which is similar to the one at the wing edge. The two rolling off mechanisms had a very distinct tendency to merge when observed at a point far from the wing. (Figure 2.2.3.1.) The corresponding circulation distribution is also shown. In this case, we show an example of a model of the wing tip which results in a rolling off which breaks down more rapidly (Figure 2.2.3.2.) compared with the one at the extreme point on the flap.

Using the same program, it is possible to analyze the problem of flap interruption at the level of the engine for a twin engine Mercury type aircraft. This problem will be of interest for the lift and the stability properties of the entire aircraft (see Chapter 3).

Figure 2.2.3.3. shows the rolling off mechanism of the vortex sheet as well as the circulation distribution over the span. The circulation is very realistic, but other calculations involving a larger number of checkpoints make it possible to modify the curve at the engine level. It seemed that the edges of the "circulation hole" are lowered. At the same time, the background becomes more hollow. The type of meshing procedure considered is very important for these phenomena. It is necessary to have continuity of the height of the square elements and in the position of the checkpoints.

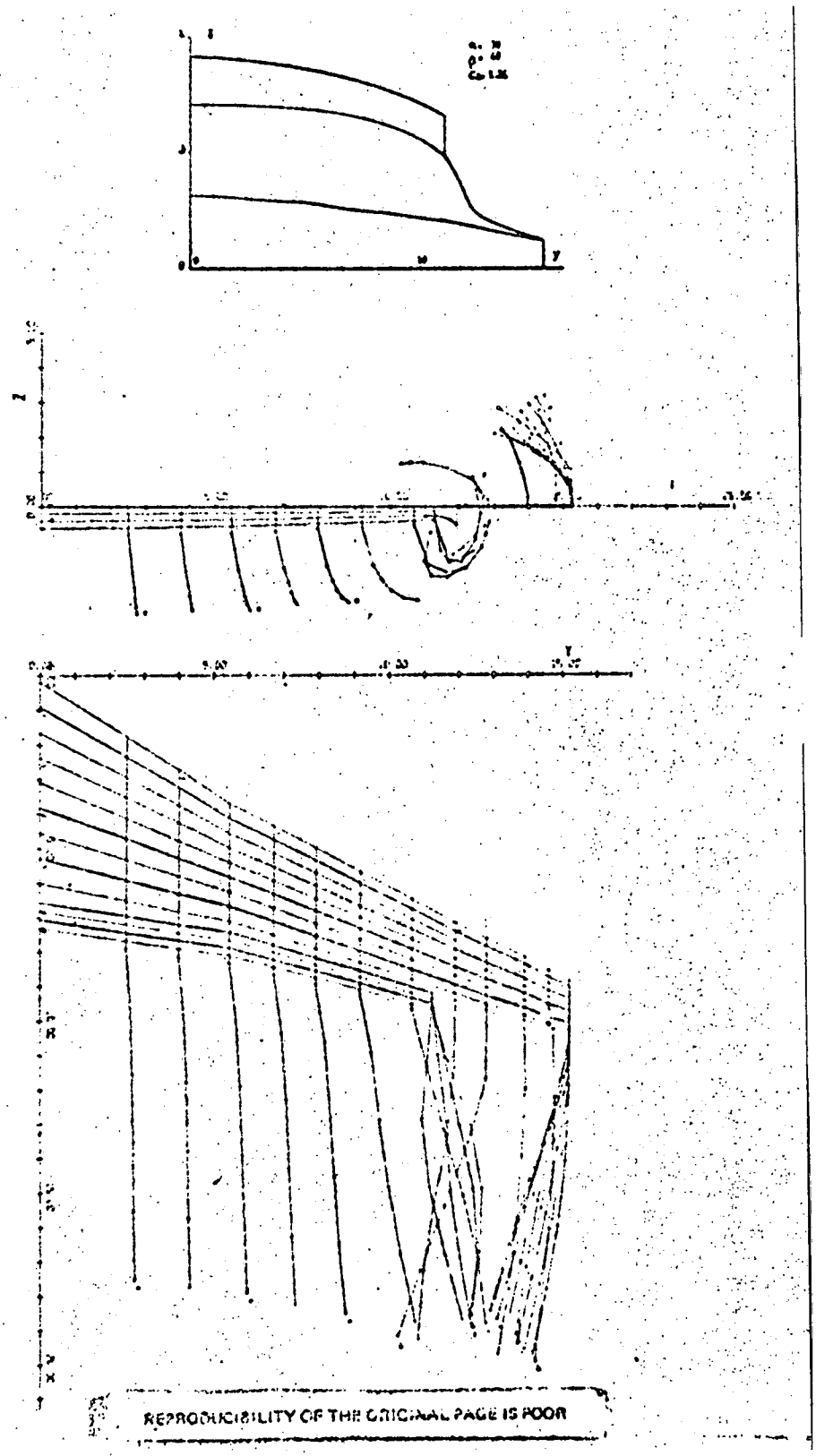

Figure 2.2.3.1. Mercury type wing with a wing flap set at 40°, incidence 10°.

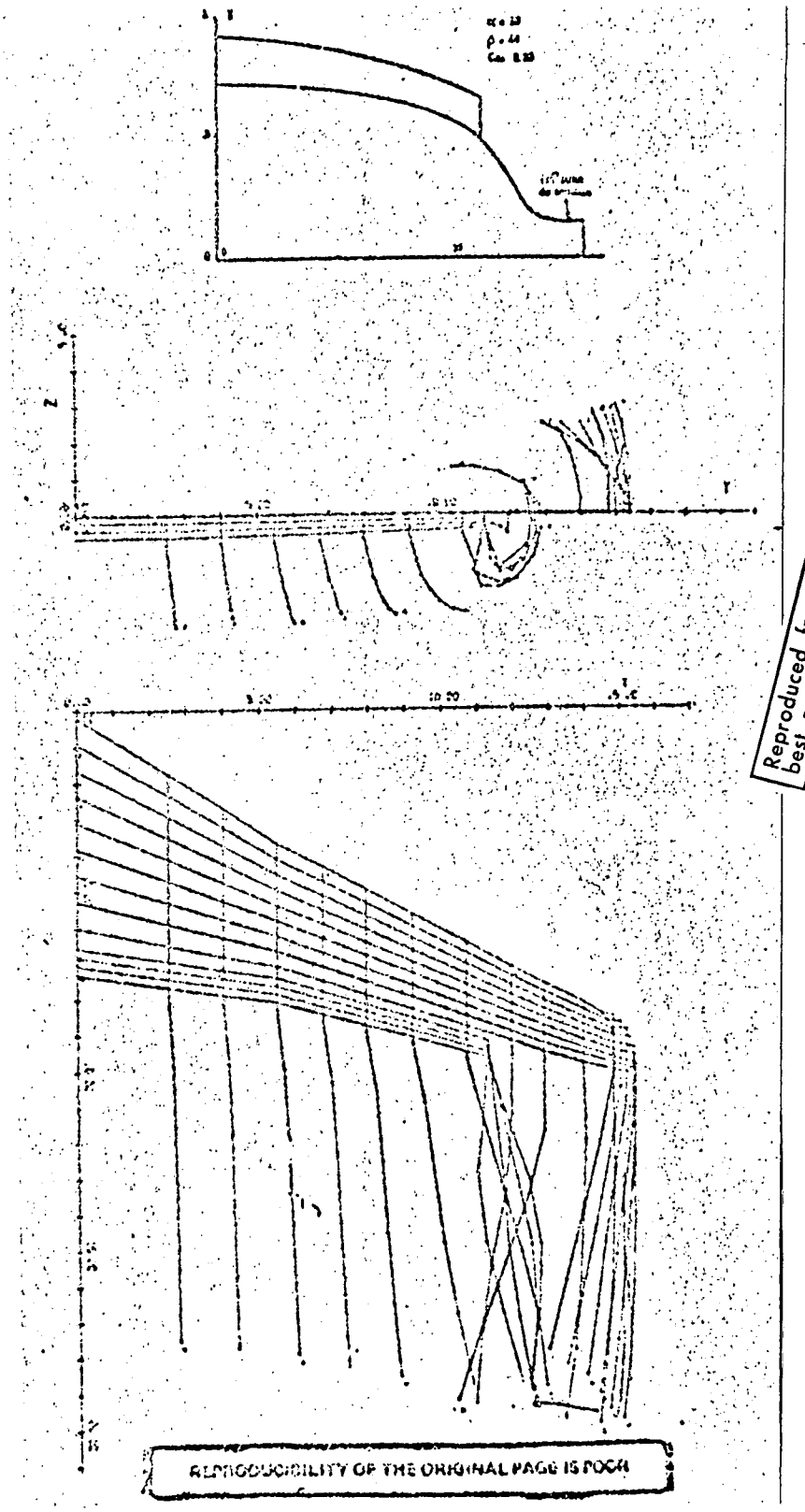

Reproduced from best available copy.

REPRODUCIBILITY OF THE ORIGINAL PAGE IS POOR

Figure 2.2.3.2. Wing with wing flap, incidence 10°.

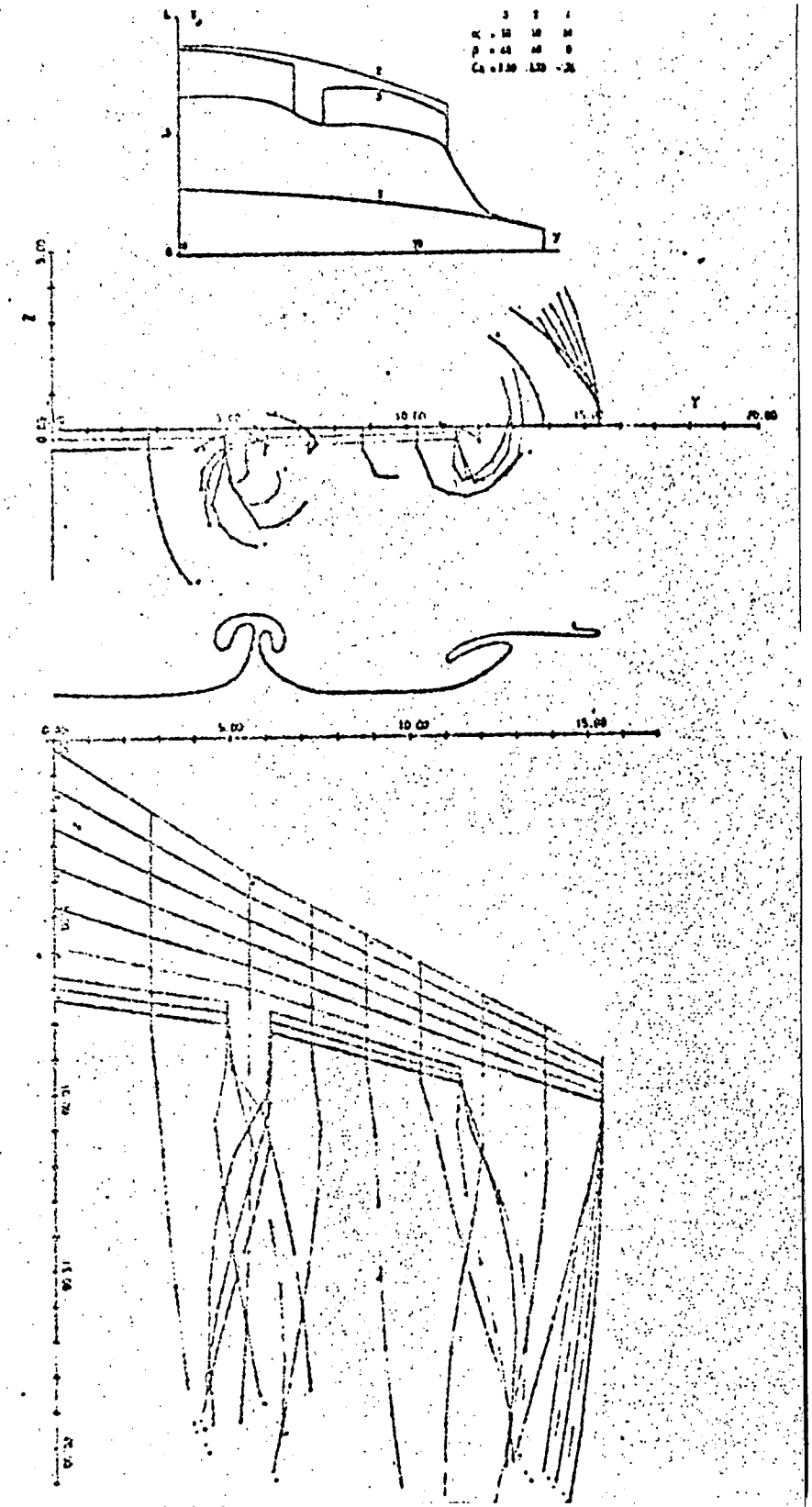

Figure 2.2.3.3. Mercury type wing with two wing flaps, set at 40°, incidence 10°.

As an example, we give the shape of the wake far behind the aircraft (Figure 2.2.3.3.).

Figure 2.2.3.4. shows various views obtained on an IBM 2250 terminal of a Mercure type wing. It shows the details of the rolling off mechanism at the extreme points of the wing and of the flaps. The corresponding circulation distribution is shown in Figure 2.2.3.5.

2.3. Calculation of the Induced Drag

/14

The method of calculation used in the preceding examples does not make it possible to obtain the value of the induced drag. We therefore also developed a method of calculation based on the energy contained in the vortex sheet. This method has the advantage of obtaining a total balance of this drag including the influence of the non-linear lift contributions. Therefore, we simply attempt to calculate the limit of $C_x = \frac{1}{S} \oint \varphi \frac{\partial \varphi}{\partial n} ds$ (ϕ is the velocity potential) when we follow the vortex sheet to infinity downstream. It seems that at a distance of one span behind the wing, a sufficiently accurate value is reached. The accuracy is primarily connected with the fact that the rolling off curve is not sufficiently known. This requires a calculation of the rolling off of a large number of discrete vortices.

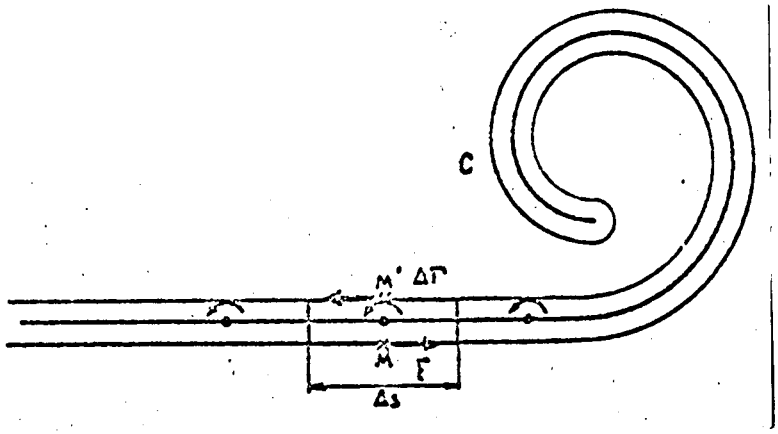

The calculation is done in two parts. We first determine the velocity potential along the integration contour C using the equation:

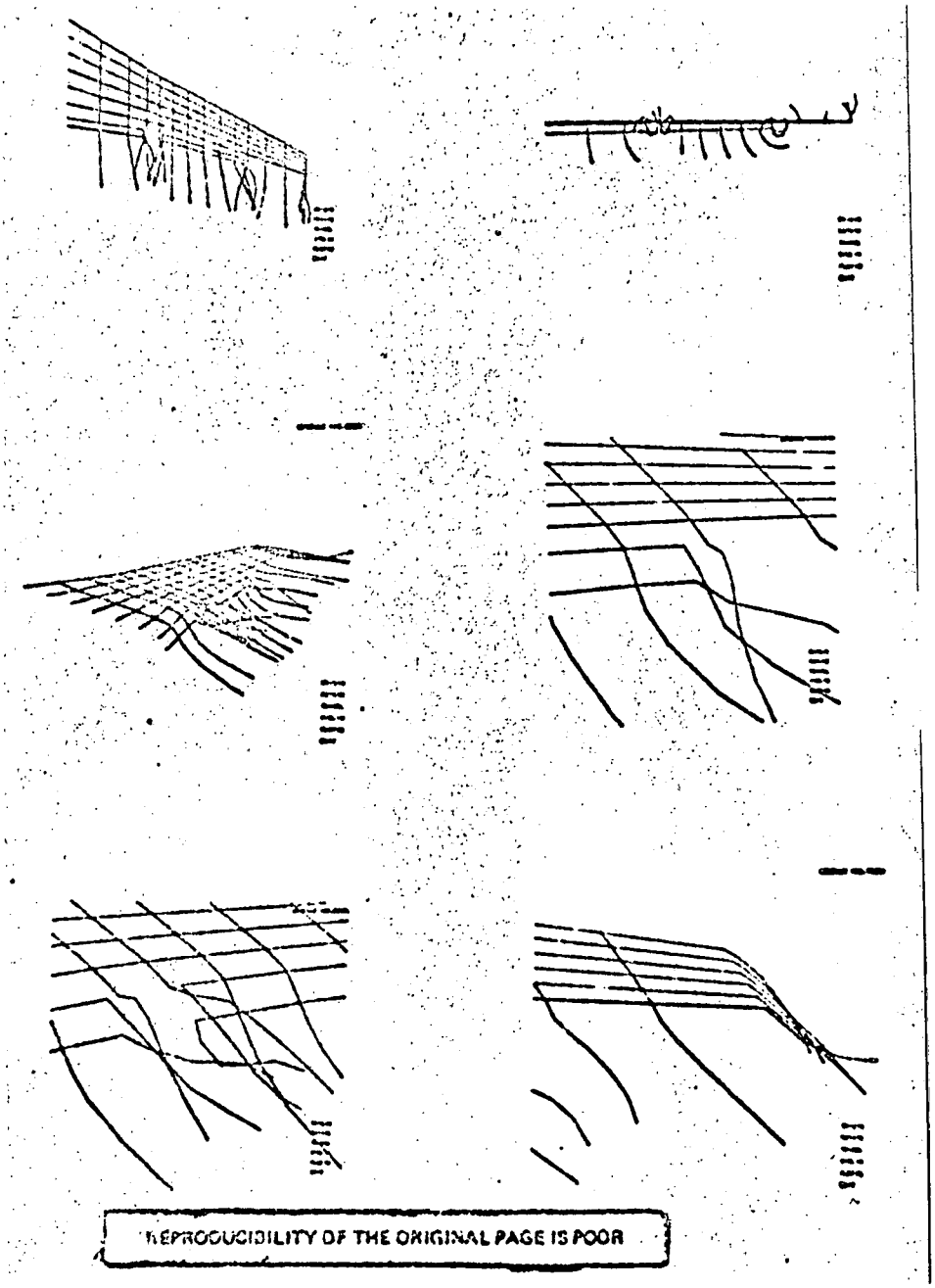

Figure 2.2.3.4. Vortex sheet generated by a Mecury type wing (IBM 22.50 terminal).

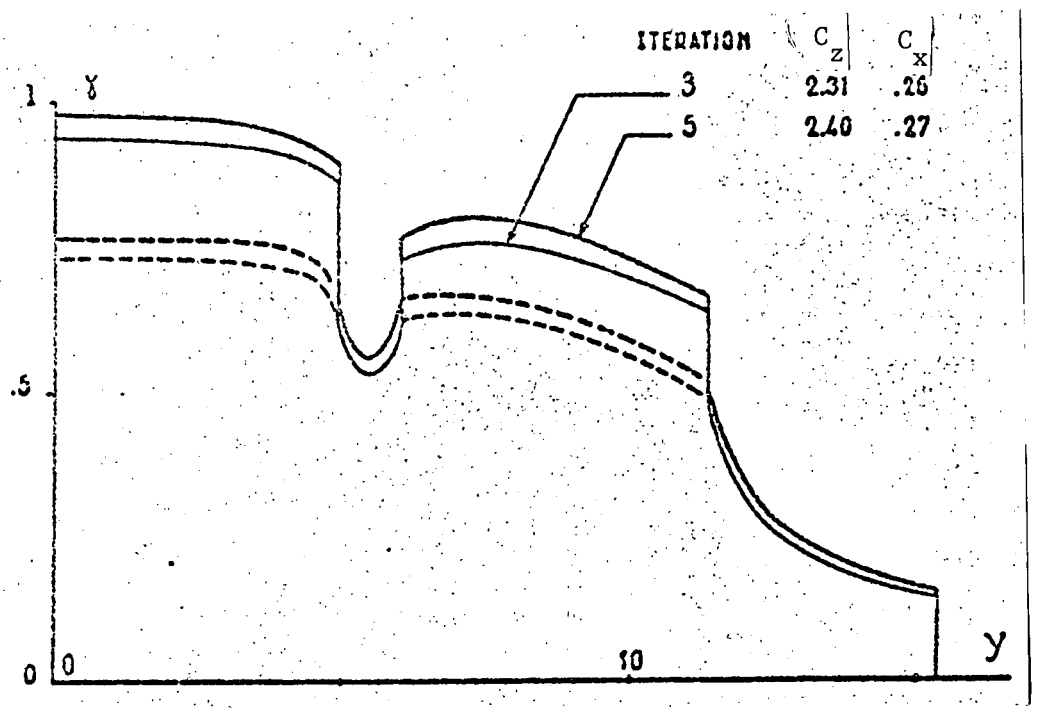

Figure 2.2.3.5. Circulation distribution over the span, Mecury type wing, incidence 10°, setting 40°.

$$\varphi = \Sigma \vec{W} \cdot \vec{\Delta s}$$

The velocity vector $\vec{W}$ is calculated at each point M by means of

$$\vec{W} = \vec{U} + \Sigma_{j \neq i} \Delta\vec{\omega} + \frac{\Delta \Gamma}{2\Delta s} \vec{t}$$

Then the calculation of the drag becomes possible by evaluating the normal derivative $\frac{\partial \varphi}{\partial n}$ along C and integrating it step by step. /15

This method was tested for an elliptical distribution. The accuracy of the result depends directly on the representation of the wing extremity and of its singularity of $\frac{d\Gamma}{dy}$.

The result can be determined to within about 10% of the theoretical value without any particular precautions. The escape of the vortices at the wing tip makes it possible to have a more realistic result.

A simplified calculation [2, 5] gives an idea of the influence of the rolling up of the sheet on the drag coefficient.

Let us consider an elliptical distribution. First we will consider a structuring of the vortices in such a way that they form a planar and deflected sheet. The following value is obtained for the aerodynamic resultant:

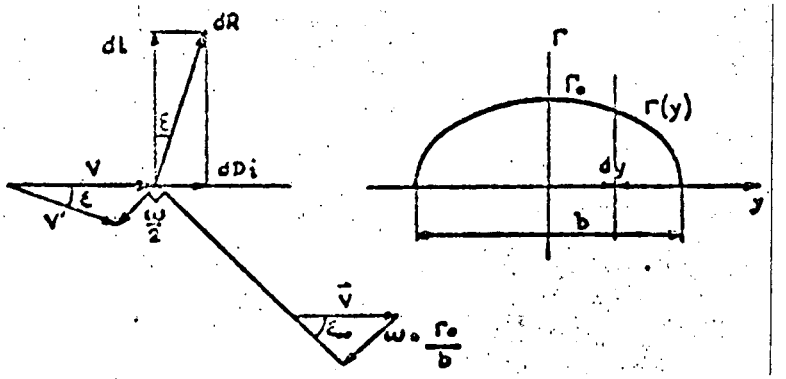

$$R = \int_{-\frac{b}{2}}^{\frac{b}{2}} \rho V' \Gamma dy = \frac{\pi}{4} \rho b \Gamma_0 V'$$

and the following is obtained for the induced drag

$$Di = R \sin \varepsilon = \frac{\pi}{4} \rho b \Gamma_0 V' \sin \varepsilon$$

$$= \frac{\pi}{4} \rho b \Gamma_0 \frac{\omega}{2} \cos \varepsilon_0$$

$$= \frac{\pi}{8} \rho \Gamma_0^2 \sqrt{1 - \frac{\Gamma_0^2}{b^2 V^2}}$$

$$Di = \frac{\pi}{8} \rho b^2 V^2 \gamma_0^2 \sqrt{1 - \gamma_0^2} = \frac{1}{2} \rho S V^2 CDi$$

We obtain:

$$CDi = \frac{\pi}{4} \lambda \gamma_0^2 \sqrt{1 - \gamma_0^2}$$

Let us now consider the case of a completely rolled up vortex sheet, described by two vortices. This case corresponds to complete rolling up very far behind the air foil. /16

The deflection W at infinity will be different and is given by the equation

$$w = \frac{2}{\pi^2} \frac{\Gamma_0}{b}$$

We now obtain

$$Di = E \cos \varepsilon_s$$

$$= \frac{\Gamma}{\delta} \rho \Gamma_0^2 \sqrt{1 - \frac{4}{\pi^2} \frac{\Gamma_0^2}{b^2 V^2}}$$

$$Di = \frac{\Gamma}{\delta} \rho b^2 V^2 \gamma_0^2 \sqrt{1 - \frac{4}{\pi^2} \gamma_0^2} = \frac{1}{2} \rho S V^2 C_{Di}$$

$$\rightarrow C_{Di} = \frac{\Gamma}{4} \lambda \gamma_0^2 \sqrt{1 - \frac{4}{\pi^2} \gamma_0^2}$$

For small values of γ_0, we find the results of the Prandtl theory

$$C_L = \frac{\Gamma}{2} \lambda \gamma_0$$

$$C_{Di} = \frac{\Gamma}{4} \lambda \gamma_0^2 = \frac{C_L^2}{\pi \lambda}$$

Figure 2.3. shows the variation of Cx as a function of α for different cases of rolling up. Unfortunately, we have not a single experimental result for comparison.

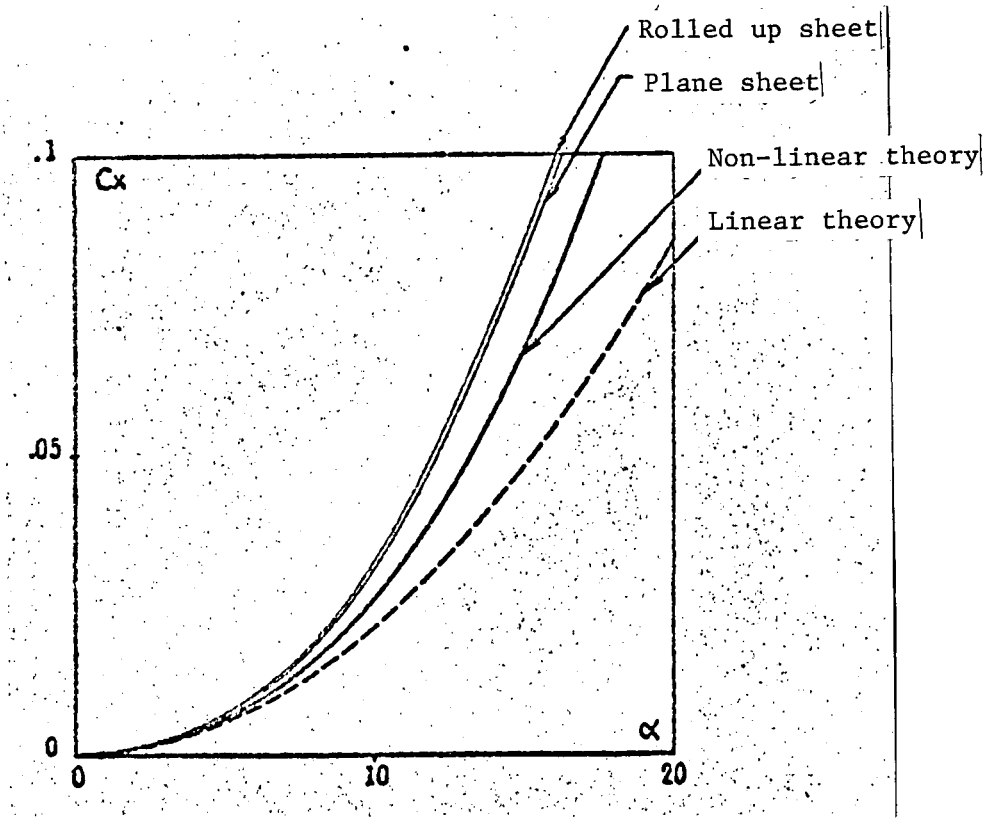

Figure 2.3. Curve for the drag coefficient as a function of incidence, flat plate of aspect ratio 1.

3. PROBLEM OF THE INTERACTION OF THE VORTEX SHEET AT THE EMPENNAGE /17

3.1. Vortex Sheet at the Level of the Empennage

Our goal is to define the geometry of the vortex sheet and to study the velocity fields induced on the empennage which could modify the moment curve Cm (i) of the aircraft in the take off or landing configuration. The rolling off of the sheet can be produced by a flap discontinuity or by local separation.

Known results refer to a rolling up at the wing tip.

This rolling up is finished at a distance behind the wing equal to approximately ten times the chord. The center line is deflected towards the bottom by an angle equal to 1 or 2° for zero incidence.

The two edge vortices have a tendency to approach each other.

It is not necessary to carry out an exact calculation when the vortices start to roll up or to find their exact position with respect to the airfoil, because this calculation is carried out in section * 2 for each angle of the incidence using the iteration method. In order to obtain a realistic velocity field at the empennage, it is sufficient to start with a circulation distribution which is properly corrected and to carry out the iteration only for the vortex sheet.

The connected vortices are located along a line at one-quarter chord.

The location of the free vortices depends on the value of the derivative $d\Gamma/dy$ and its discontinuities. /18

*Translator's Note: Words missing in foreign text.

The program follows the vortex checkpoints where the influence of all the vortices is calculated, and where the new trajectory of the sheet is determined.

This method was tested in the simple case of an elliptical wing. The example due to Westwater [4] was used again by introducing vortices with constant $\Delta\Gamma$. We obtained the same type of rolling up (Figure 3.1.1). It was then applied to the Mercury wing.

We started with a small number of vortices and made our model more complicated to an increasing degree in order to approach the conditions on a real airfoil. We started the study with a configuration having a continuous wing flap. This first model showed a rolling up at the level of the flap discontinuity. Nevertheless, this rolling up is far from being complete at the empennage level. Figure 3.1.2 shows the interaction of the wake with the empennage.

In order to simulate the vortex discontinuity in a better way, we added vortices which escape at the flap edge, corresponding to the discontinuity of $d\Gamma/dy$.

Figure 3.1.2 shows the results of this representation. The curve of iso $X = X_{empennage}$ shows the configuration before rolling off. It simulates the flow at the flap edge with sufficient accuracy. /19

We will now consider the more realistic case of an airfoil having wing flaps with flap discontinuities at the location of the engine. Figure 3.1.3 shows the rolling off at the flap edge very well.

Figure 3.1.4 shows the case of a Mercury wing with jet flaps in which the influences of the pylon and of the engine nacelle can be seen.

The discontinuities of $d\Gamma/dy$ are sources where the rolling off begins. However, the rolling off never is complete at the empennage level.

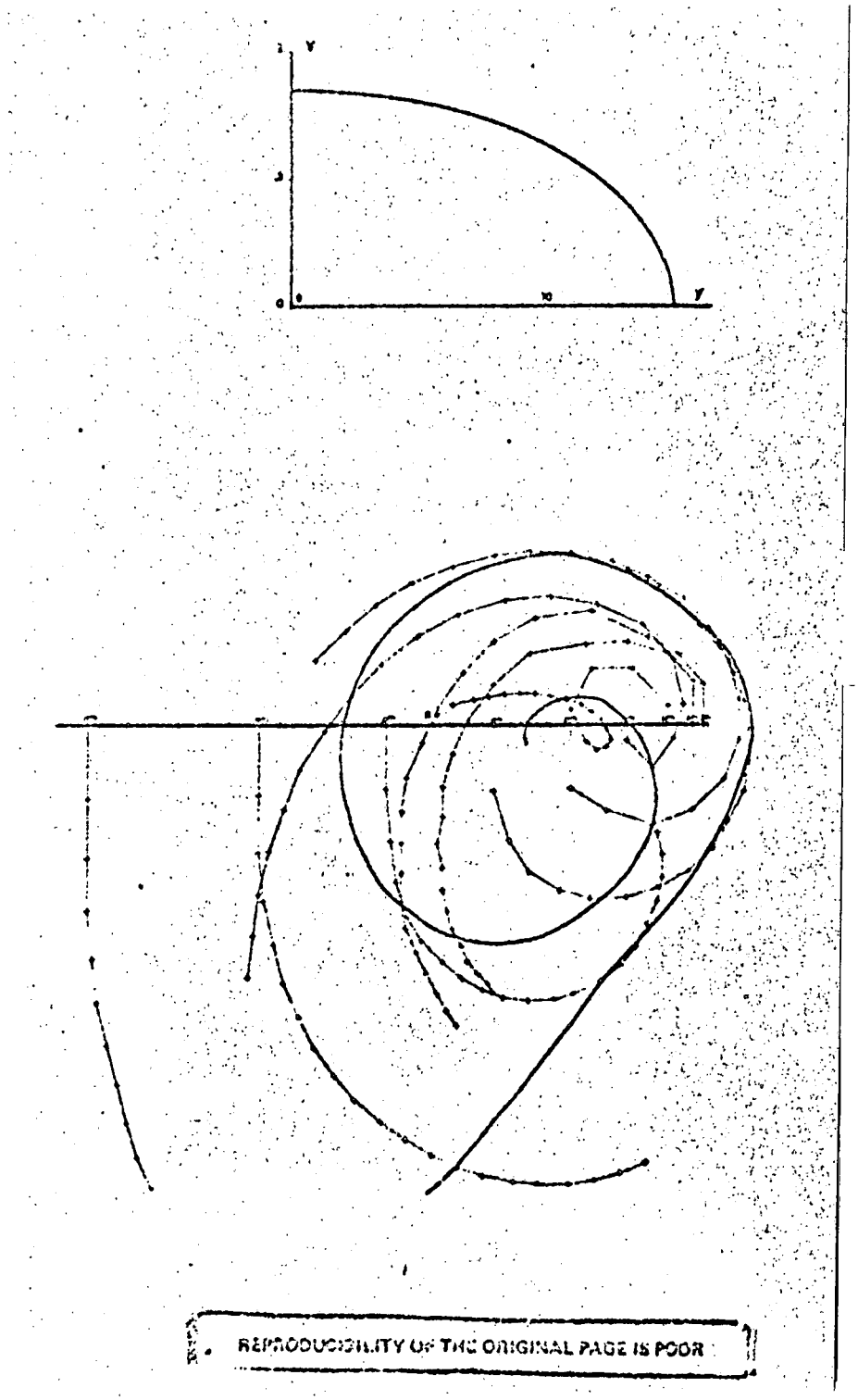

Figure 3.1.1. Elliptical rolling up.

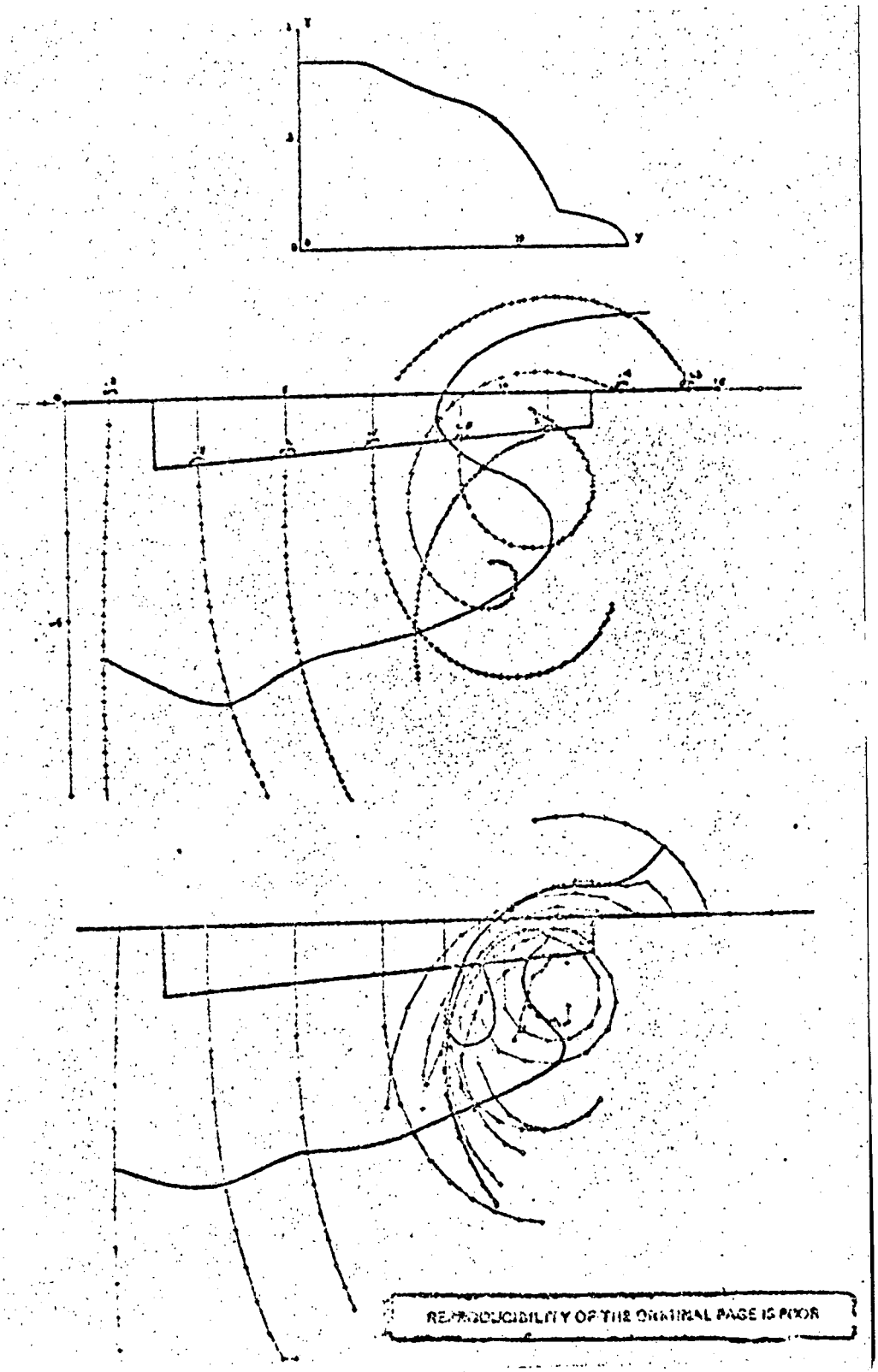

Figure 3.1.2. Wing with a flap.

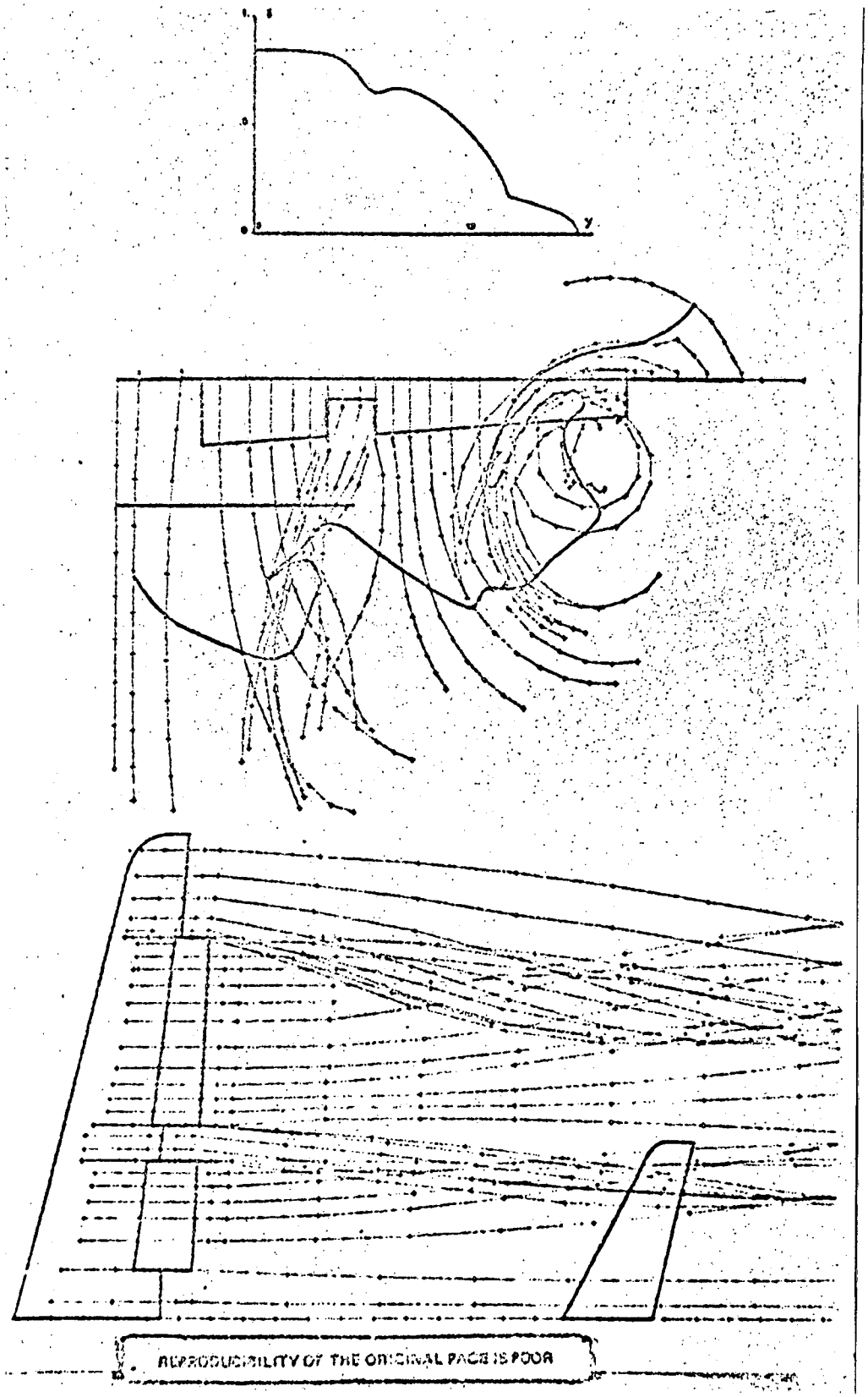

Figure 3.1.3. Wing with wing flaps.

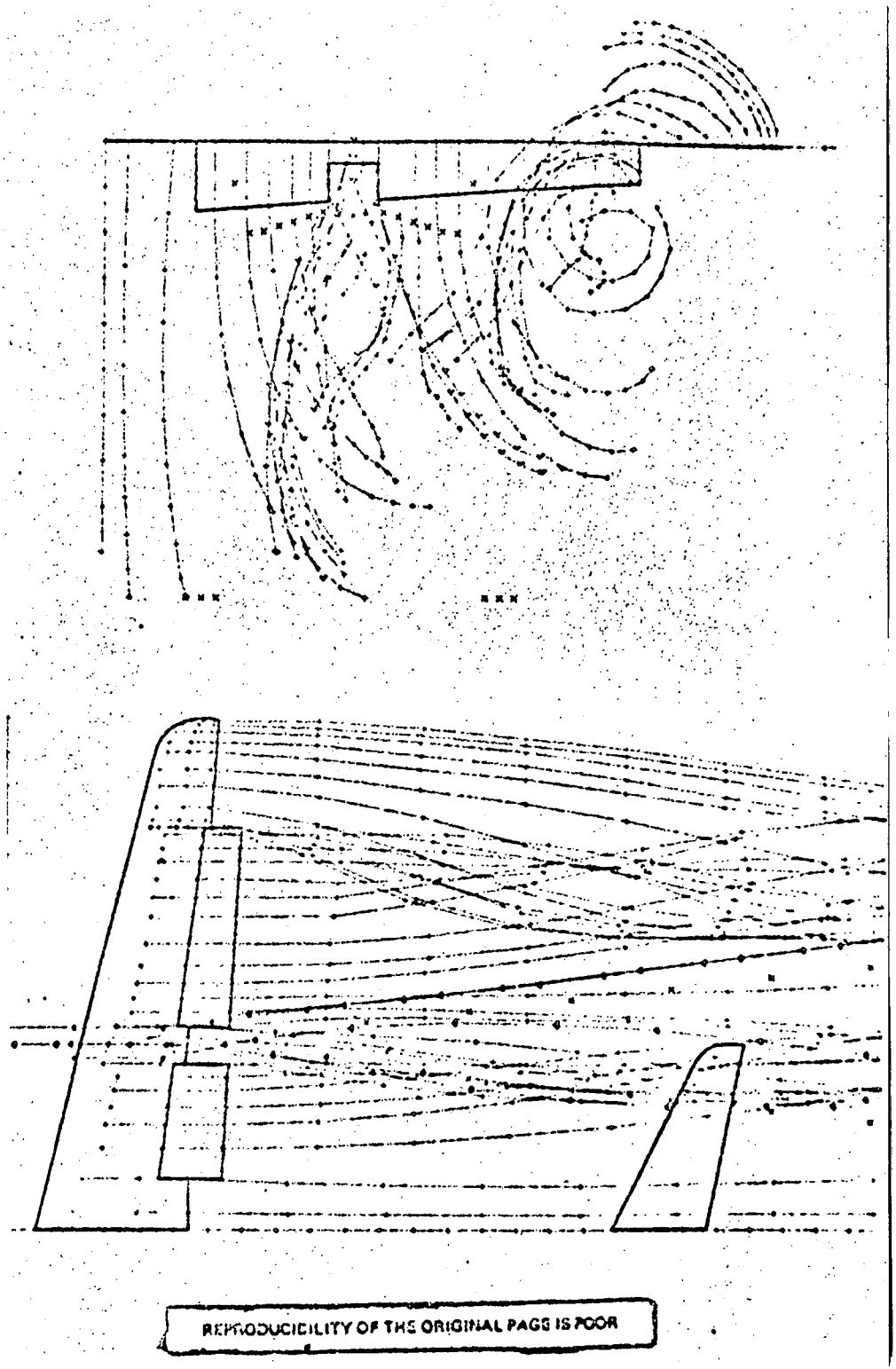

Figure 3.1.4. Wing equipped with flaps, a pylon and an engine nacelle.

If the circulation curve is continuous and closed at the discontinuities of $d\Gamma/dy$, the fact that the vortex sheet is made discrete adversely affects the method only to a very small degree.

3.2. Application

The circulation over the empennage of the aircraft can be accurately calculated from this induced velocity distribution. For example, a lifting line can be assumed. A moment introduced by the empennage is produced which is not at all linear with the incidence angle. Instead it is a function of the distance from the vortex sheet to the empennage, its shape and also the manner in which this sheet is rolled up. Figure 3.2.1 shows a photograph of the IBM 2250 graphic terminal screen. This screen is being used as an interface between the engineer and the computer for a large part of theoretical aerodynamics problems which are in the evaluation stage. It is used for displaying aerodynamic solutions, as well as to carry out iteration calculations which are controlled by the engineer. (Figure 3.2.1).

In this report, the engineer modified the geometry (size, /20
dihedral, position) of the empennage in order to find their influence on the stability curves of the complete aircraft. He also wants to see the modifications for several configurations with the wing upstream. This means that these complex problems can be grasped and optimized rapidly. The engineer rapidly finds the meaning of the important parameters in any study he is carrying out. This makes it possible for him to define areas where compromises are needed and which must be either calculated by a detailed method or tested in the wind tunnel.

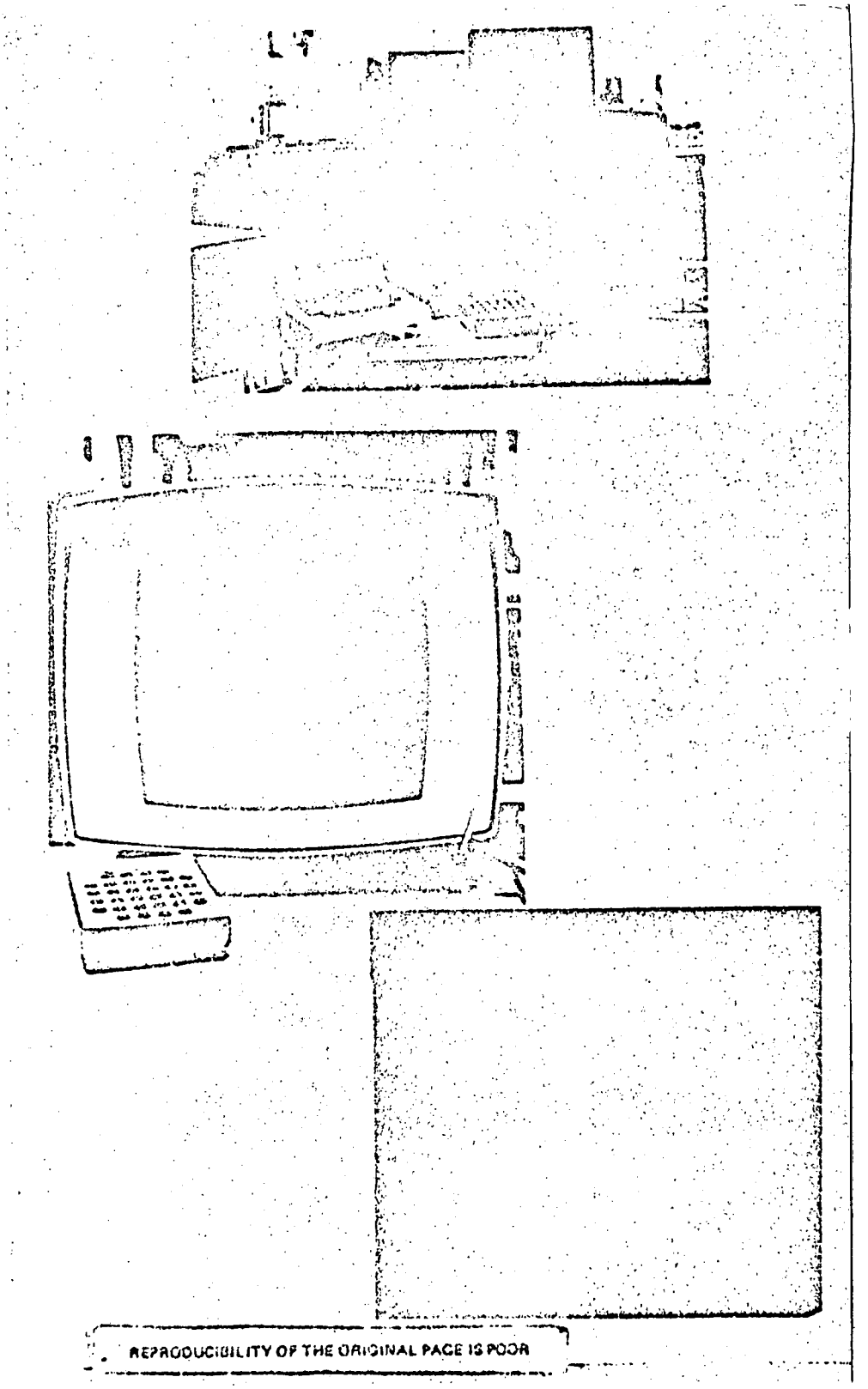

Figure 3.2.1. Engineer-computer interface.

REFERENCES

1. Bielotzerkovskiy, C. M. Calculation of the Flow Around Planar Wings of Arbitrary Shape for a Large Incidence Range. Akademii Nauk SSSR, 1968.

2. Spreiter, J. R. and Alvin H. Sacks. Rolling up of the Trailing Vortex Sheet and its Effect on the Downwash Behind Wings. Journal of the Aeronautical Sciences, 1951.

3. Legendre, R. Cone Shaped Sheets at the Leading Edges of a Delta Wing. ONERA, Recherche Aerospatiale, 1959.

4. Westwater, F. L. Rolling up of the Surface of Discontinuity Behind an Airfoil of Finite Span. Aeronautical Research Committee, 1935.

5. Sato, H. and K. Matsuoka. On Limit of Circulatory Lift on Wings with Finite Span, AIAA.

Translated for National Aeronautics and Space Administration under Contract No. NASw 2035, by SCITRAN, P.O. Box 5456, Santa Barbara, California 93108.